Hybrid Aptamer–Antibody Linked Fluorescence Resonance Energy Transfer Based Detection of Trinitrotoluene

ARTICLE *in* ANALYTICAL CHEMISTRY · JULY 2014

Impact Factor: 5.64 · DOI: 10.1021/ac501388a · Source: PubMed

7 AUTHORS, INCLUDING:

Dr. Priyanka
Institute of Nano Science and Technology
24 PUBLICATIONS **261** CITATIONS
SEE PROFILE

Preeti Singh Pathania
Institute of Microbial Technology
3 PUBLICATIONS **10** CITATIONS
SEE PROFILE

Vijayender Bhalla
Institute of Microbial Technology
30 PUBLICATIONS **371** CITATIONS
SEE PROFILE

CR Suri
Institute of Microbial Technology
78 PUBLICATIONS **1,376** CITATIONS
SEE PROFILE

analytical chemistry

Letter

pubs.acs.org/ac

Hybrid Aptamer-Antibody Linked Fluorescence Resonance Energy Transfer Based Detection of Trinitrotoluene

Priyanka Sabherwal,[†,∥] Munish Shorie,[‡,∥] Preeti Pathania,[‡] Shilpa Chaudhary,[‡] K. K. Bhasin,[§] Vijayender Bhalla,[‡] and C. Raman Suri*[,‡]

[†]Institute of Nano Science and Technology, Sector 64, Mohali 160064, India

[‡]CSIR-Institute of Microbial Technology, Sector 39-A, Chandigarh 160036, India

[§]Department of Chemistry, Panjab University, Chandigarh 160014, India

Supporting Information

ABSTRACT: Combining synthetic macromolecules and biomolecular recognition units are promising in developing novel diagnostic and analysis techniques for detecting environmental and/or clinically important substances. Fluorescence resonance energy transfer (FRET) apta-immunosensor for explosive detection is reported using 2,4,6-trinitrotoluene (TNT) specific aptamer and antibodies tagged with respective FRET pair dyes in a sandwich immunoassay format. FITC-labeled aptamer was used as a binder molecule in the newly developed apta-immunoassay format where the recognition element was specific anti-TNT antibody labeled with rhodamine isothiocyanate. The newly developed sensing platform showed excellent sensitivity with a detection limit of the order of 0.4 nM presenting a promising candidate for routine screening of TNT in samples.

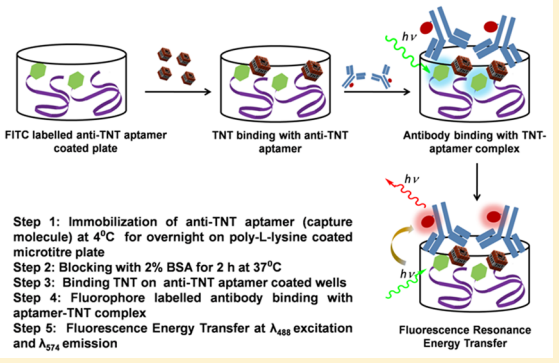

The detection of nitro-explosive 2,4,6-trinitrotoluene (TNT) is an important environmental, security, and health concern for the global community because of its widespread contamination due to its extensive use, storage, testing, and disposal.[1] TNT enters the environment from manufacturing, processing, and destruction of bombs and grenades, including recycling of explosives. The different military and terrorist activities have resulted in extensive contamination of soil and groundwater by TNT.[2] The current methods of detecting TNT residues are commonly performed off-site and involve complex instrumentation such as mass spectrometry, ion mobility spectrometry, gas or liquid chromatography, and surface acoustic wave methods.[3] Currently, detection strategies are trended toward development of field applicable and portable techniques which are reliable and sensitive enough to evaluate the presence of TNT in field conditions such as chemosensors and biosensors.[4−7] More commonly, fluorescence resonance energy transfer (FRET) based assays are being reported and becoming decisively established tools for the detection and quantification of explosive contaminants[8−10] because of their simplicity in assay design and operation. In this nonradiative process, an excited state donor (usually a fluorophore) transfers energy to a proximal ground state acceptor through long-range dipole−dipole interactions. The rate of energy transfer is highly dependent on the extent of spectral overlap, the relative orientation of the transition dipoles, and also the distance between the donor and acceptor molecules (∼10−100 Å). Several groups have reported detection of explosives using fluorescence resonance energy transfer (FRET) either by using nanoparticles based self-quenching or energy transfer mechanisms.[11,12] However, most of these assay formats are subject to nonspecific response since these assays are reported without using any specific bioreceptors such as antibodies or aptamers.

Affinity based assays using specific antibodies and/or aptamers offer a preferential alternate approach for explosives detection in virtue of their high selectivity, sensitivity, and rapidness.[13−16] However, the critical part is to get high-quality bioreceptors to be used as recognition/capture molecules. This could be accomplished by using a suitable hapten, which is designed in such a way that it can mimic the structure of target molecules so as to obtain antibodies and/or aptamers having higher specificity toward the target molecule.[17,18] The present study involves the production of highly specific bioreceptor pair (antibodies and aptamers) against the target analyte, TNT, and their use in a newly antibody-antigen-aptamer structured fluorescent resonance energy transfer (FRET) based sandwich immunoassay format.

Aptamers have been utilized as antibody alternatives, functioning in a similar fashion with molecular recognition as a target biomarker as they mimic the properties of antibodies in a variety of diagnostic formats.[20,21] The developed aptamers were labeled with fluorescein isothiocyanate (FITC) and were

Received: April 16, 2014
Accepted: July 10, 2014
Published: July 10, 2014

   dx.doi.org/10.1021/ac501388a | *Anal. Chem.* 2014, 86, 7200−7204

used as a binder molecule in the newly developed FRET apta-immunoassay format (Figure 1) where the recognition element

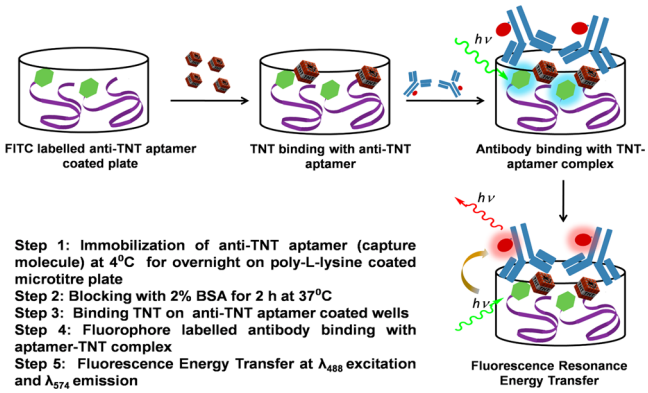

Figure 1. Schematic showing aptamer-antibody linked FRET apta-immunoassay for TNT detection in sandwich format.

was specific anti-TNT antibody labeled with rhodamine isothiocyanate (RITC). Specific anti-TNT antibody and aptamers were produced in-house by using a suitable hapten-protein conjugate. For this, 2,4,6-trinitrometatoluidine (TNMT), analogue of TNT, was selected based on minimum energy confirmations studies using geometry optimization modules in ChemBio 3D 11.0 and Hyperchem 8.0. To preoptimize the structures, molecular mechanics force field MM2 was used (ChemBio3D, minimum rms ~0.042 kJ mol $Å^{-1}$). Quantitative structure−activity relationship (QSAR) studies were carried out on the basis of the energy-minimized structures using QSAR descriptors such as molecular surface area/volume, dihedral angle, polarizability, hydration energy, log of the octanol/water partition coefficient (log *P*), refractivity, the lowest unoccupied molecular orbital energy (E_{LUMO}), the highest occupied molecular orbital energy (E_{HOMO}). The graphical representation of E_{HOMO} and E_{LUMO} for TNT and TNMT indicated that the nitro groups are likely to be an important portion of the TNT epitope for antibody recognition (Supporting Information, Figure S1). The well characterized hapten was further conjugated to a carrier protein (BSA) (Supporting Information, Figure S2) and used successfully in the production of specific anti-TNT antibodies. A relatively good titer (1×10^{-6}) of anti-TNT antibodies was obtained with conjugate, prepared at the optimum hapten/protein molar ratio (1:30) with an IC_{50} value equal to ~0.1 ng mL^{-1} (Supporting Information Figure S3).

Similarly, aptamers specific to the target molecule (TNT) were identified through an *in vitro* process employing the modified SELEX method as reported earlier in our previous study.[19] The screening of binders was initiated from the high-pressure liquid chromatography (HPLC) purified ssDNA library of 52 nucleotides (nt, random region) flanked by 18-nt fixed region for polymerase chain reaction (PCR) amplification. Amplification of ssDNA pool was performed with FITC labeled primer (forward) and biotin labeled primer (reverse). The oligomers from the library were exposed to the hapten-protein conjugate (TNMT-BSA) and the specific binders were eluted and pooled for subsequent SELEX rounds. The complexity of the original library was reduced with the

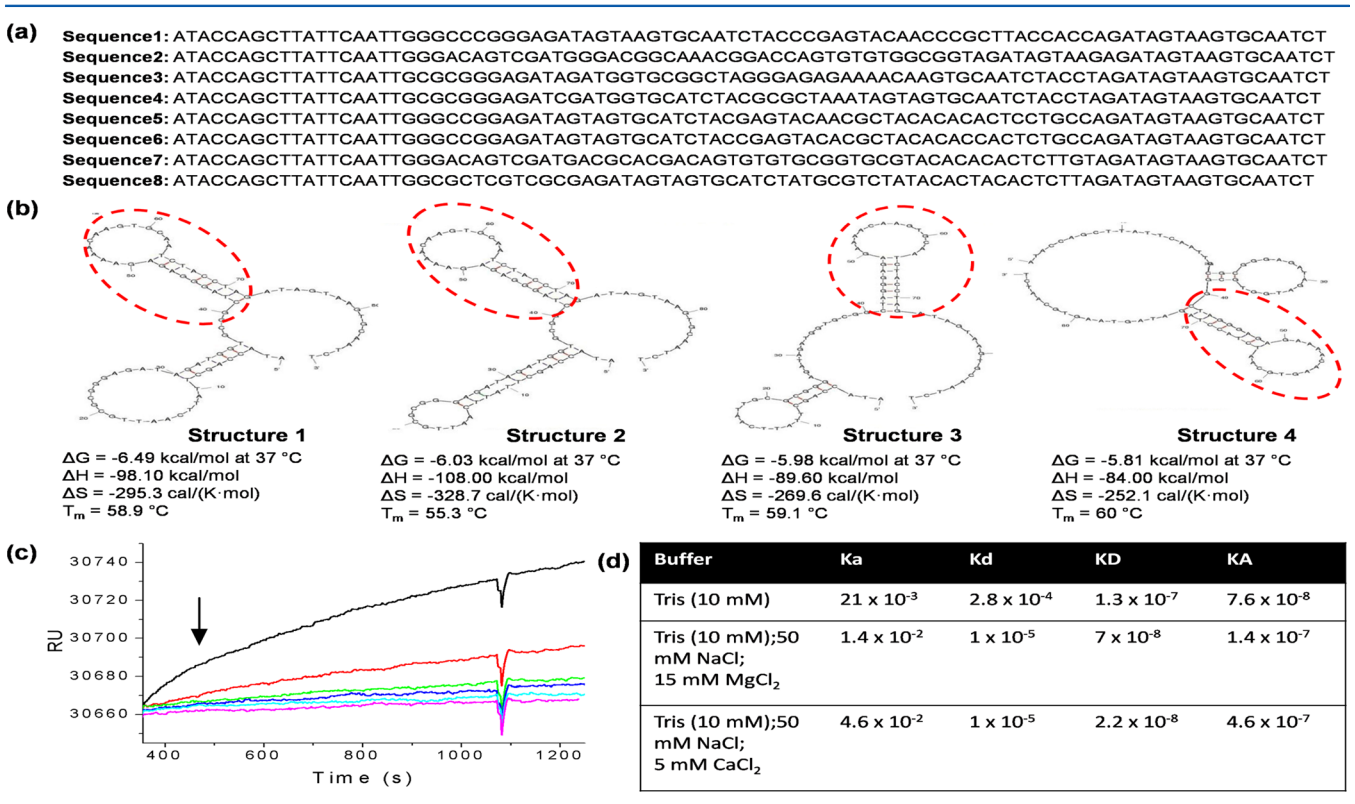

Buffer	Ka	Kd	KD	KA
Tris (10 mM)	21×10^{-3}	2.8×10^{-4}	1.3×10^{-7}	7.6×10^{-8}
Tris (10 mM);50 mM NaCl; 15 mM $MgCl_2$	1.4×10^{-2}	1×10^{-5}	7×10^{-8}	1.4×10^{-7}
Tris (10 mM);50 mM NaCl; 5 mM $CaCl_2$	4.6×10^{-2}	1×10^{-5}	2.2×10^{-8}	4.6×10^{-7}

Figure 2. (a) Seven prospective aptamer sequences obtained through the modified SELEX method.[19] (b) The predicted secondary structures of selected sequence-1 and the corresponding thermodynamical parameters obtained from the mfold Web server http://mfold.rna.albany.edu/?q=mfold. (c) Kinetic studies showing an overlay of SPR sensograms. Arrow depicts the decreasing concentration of aptamers from 0.001 to 100 nM, respectively (d) Affinity parameters of synthesized aptamer sequence-1 under optimum buffer conditions.

dx.doi.org/10.1021/ac501388a | *Anal. Chem.* 2014, 86, 7200−7204

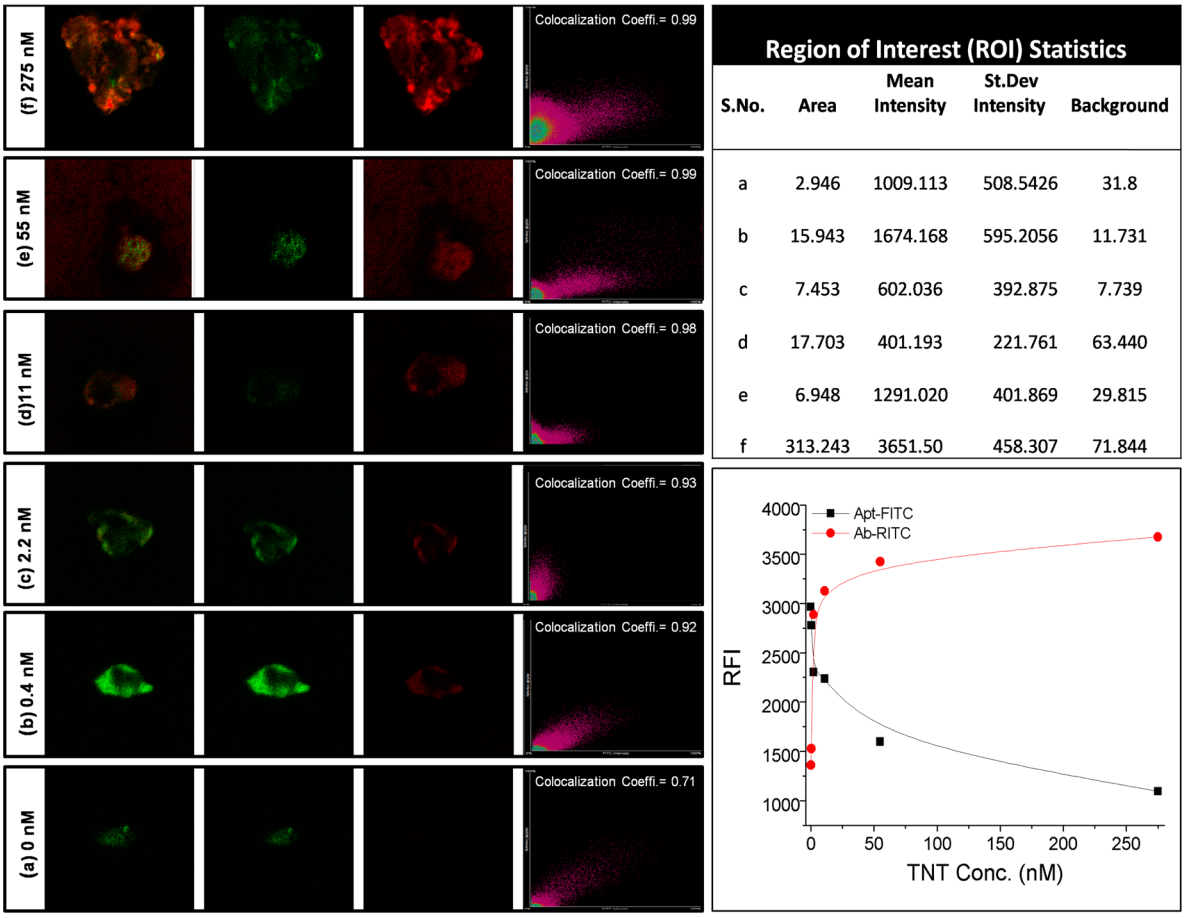

Figure 3. Confocal micrographs showing quantification of fluorescence intensity in sandwich FRET apta-immunoassay format. Specific FITC-TNT aptamer (5 nM) immobilized on the poly-L-lysine coated chamber slide incubated with varying concentrations of standard TNT solutions (a–f, 0–1.375 μM) with fixed concentration of RITC labeled anti-TNT antibody (1st panel, merged image of apta-TNT-antibody complex; second panel, apta-FITC; third panel, antibody-RITC; fourth panel, degree of colocalization in the selected region of interest). The normalized quantification of fluorescence in the graph shows the change in fluorescence counts for TNT in a concentration dependent manner in the developed FRET assay. The change in ROI statistic values for each TNT concentration is shown in the ROI table.

progressive SELEX rounds thereby yielding target specific enriched pool at the end of fifth cycle. The purified PCR products were cloned into *Escherichia coli* using pTZ57R/T cloning vector having multiple cloning sites designed for mapping, screening, and excision of the cloned insert. After sequencing, seven prospective sequences were found to retain the initial library design with correct primer binding regions (Figure 2a). Their alignment led to the identification of three sequence families in seven individual aptamer clones as can be seen in the cladogram tree (Supporting Information, Figure S4a), indicating the convergence of potential aptamers in the resulting pool.

Selected ssDNA molecules were subjected to secondary structure prediction using the mFold software (Supporting Information, Figure S4b) at 27 °C in 100 mM [NaCl] and 15 mM [$MgCl_2$]. The parameters for mfold were set to default which allowed for a broad variety of predicted secondary structures. On the basis of maximum stability and predicted energy values, sequence-1 was selected for further analysis (Figure 2b). In the predicted secondary structure, a 32 nucleotide hairpin substructure (encircled red) near the 3′ end is present in each substructure showing its pervasiveness demonstrating its stability and affinity toward target analyte (Supporting Information, Figure S5). One-dimensional ^{1}H NMR for DNA structure validation further confirmed the molecular symmetry in the ssDNA substructure (Supporting Information, Figure S6). NMR signals of the backbone amides provide two probes to monitor complex formation: extreme resonance line broadening and chemical shift perturbation.[22] The identified consensus motif was further analyzed for its affinity toward the target analyte TNT by surface plasmon resonance (SPR) analysis using the as prepared TNMT-BSA conjugate on the carboxymethylated dextran (CM-dextran) SPR chip. Kinetic studies showing overlay of SPR sensograms (Figure 2c) obtained for TNT specific aptamer using varying concentrations from 0.001 to 100 nM. The effect of divalent ions on the affinity of selected aptamer sequence by using Tris buffer spiked with $MgCl_2$ and $CaCl_2$, respectively, was investigated. The corresponding affinity (Figure 2d), KD values calculated from the ratio between dissociation (kd) and association (ka) were found to be highest ~2.2×10^{-8} for Ca^{2+}, since these divalent ions shows high affinity toward chelation with DNA to form respective confirmations and are more tightly bound to DNA.[22] The selected bioreceptors (both antibodies and aptamers) were employed in a newly developed sandwich apta-immunoassay format. The confocal microscopy studies were carried out using a Nikon AI-R laser scanning confocal microscope to visualize and quantify FRET measure-

dx.doi.org/10.1021/ac501388a | *Anal. Chem.* 2014, 86, 7200–7204

ments simultaneously in the selected region of interest. FITC-TNT aptamer (5 nM) immobilized on the poly-L-lysine coated chamber slide was incubated with varying concentrations of standard TNT solutions (a–f, 0–1.375 μM) followed by adding a fixed concentration of RITC labeled antibodies (5 μg mL^{-1}). The apta-TNT-antibody complex in the sandwich format was viewed by exciting at 405 nm with a laser source, and the images were acquired by collecting emitted light at 565 nm, the characteristic emission of RITC-antibodies. Imaging was performed using a 512 × 512 pixel size and 16 scans were selected per image. Figure 3a–f shows the related increase in fluorescence intensity of the acceptor (RITC-Ab) and concomitant decrease in the intensity of the donor (FITC-apt) with increasing concentrations of TNT. The degree of colocalization in micrographs exhibited the change in the colocalization coefficient from 0.7 to 0.99 indicating the efficient energy transfer between the donor and the acceptor due to the formation of the apt-TNT-antibody complex. The appropriate regions of interest (ROI) were visually selected for FRET imaging and their respective pixel coordinates were calculated for fluorescence measurements. Statistical analysis of the FRET response was carried out comparing the pixel intensities/μm^2 of apta-TNT-Ab complex using NIS-Elements AR 3.2 Nikon software (Figure 3, table). The quantification of the fluorescence counts for varying concentrations of TNT indicated a constant decrease in fluorescence intensity of FITC (donor) with a subsequent increase in RITC (acceptor) intensity as shown in the graph in Figure 3. The graphical representation of concentration dependent change in the respective fluorophore intensity clearly indicates the FRET phenomenon occurring between the two FRET pairs in the apta-immuno complex.

The concentration dependent quantitation of TNT in standard water samples was carried out on microtiter plates by measuring the FRET signal intensity at 560 nm, correlating the concentration of TNT. In general, sandwich-based assays have largely been employed in protein detection where enzyme-linked immunosorbent assay (ELISA) has become the standard approach. In this approach, two different antibodies, a capture antibody and a reporter antibody, both specific to the target antigen are required. Usually, the first antibody is immobilized onto a substrate and interacts with the target antigen, while the second labeled antibody reacts with the captured antigen, resulting in a sandwich format. Though widely used, this approach is restricted to the detection of large molecules only, since it is unlikely that low molecular weight molecules such as pesticides, etc. will simultaneously bind to two antibodies due to steric hindrance or being univalent in nature. For this, the development of target specific DNA aptamers was potentially explored for the detection of small molecules in a sandwich structure mode. In the newly developed apta-immuno sandwich assay format, FITC-labeled aptamer was used as a binder molecule where the recognition element was a specific anti-TNT antibody labeled with rhodamine isothiocyanate resulting in a FRET signal. DNA aptamer specific to TNT were screened by employing the nanoparticle (Au) mediated modified SELEX method (Supporting Information, Figure S7).

The selectivity of the screened aptamers was checked by employing binding studies with hapten-protein conjugates. A sandwich FRET apta-immunoassay was developed on the microtiter plate for the TNT detection. Anti-TNT antibody labeled with RITC (5 μg mL^{-1}) prepared in carbonate buffer (100 mM, pH 9.4) was added to the microtiter plate and kept for incubation overnight at 4 °C. The plate was subsequently washed thoroughly with phosphate buffer (PB) (50 mM, pH 7.2). Unbound sites in the wells of the microtiter plate were blocked with 10% defatted skimmed milk in PB for 1 h at 37 °C. After washing the plate with PB (3×), standard TNT solutions prepared in water at varying concentrations (0–6.8 μM) were added to each well followed by incubation for 2 h at 37 °C followed by washing as described previously. An optimum concentration (5 nM) of FITC labeled aptamer was then added into each well of the plate, and subsequently fluorescence counts were measured using the fluorescence microtiter plate reader (BioTek synergy, Finland) at 488 nm excitation and 560 nm emission, respectively. In the control experiments, the microtiter plates were coated with poly-L-lysine-TNT-Ab-RITC, poly-L-lysine-apt-FITC-Ab-RITC without TNT, and a nonspecific oligonucleotide-TNT-Ab-RITC. No significant signals were observed in all negative controls in comparison to a positive control using poly-L-lysine-apt-TNT-Ab-RITC complex on a microtiter plate (Supporting Information, Figure S8).

For a cross-reactivity pattern, TNT analogues (DNT and MNT, respectively) were added into the wells, and FRET measurements were carried out as described above. The assay exhibited an excellent sensitivity showing the dynamic response range from 0 to 6.8 μM for TNT and its analogues with a detection limit of ~0.4 nM (Figure 4a) for TNT. The

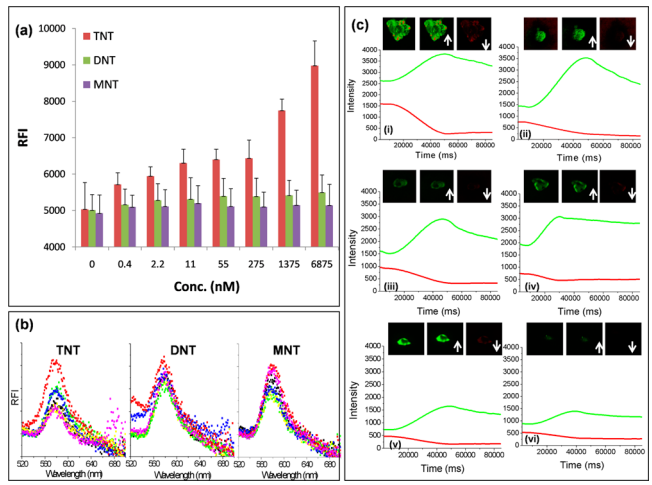

Figure 4. (a) FRET signals of increasing TNT concentrations (0–6.8 μM) in sandwich apta-immunoassay format. (b) The resulting FRET plots for TNT, DNT, and MNT for the above concentrations. Part c depicts the FRET phenomenon between apta-immuno complex with different concentrations of TNT (i–vi, 0–1.375 μM, respectively) as obtained by bleaching the donor fluorophore (Antibody-RITC). Inset of each graph (i–vi) shows the merged image of the apt-TNT-Ab complex (left panel); apt-FITC (middle panel); and Ab-RITC (right panel). The upward and downward arrows indicate the respective increase/decrease in fluorescence signal of donor and acceptor FRET pair dyes.

corresponding spectrum at different concentrations of TNT and its analogues (DNT and MNT) showed the selectivity of the newly developed assay for TNT only (Figure 4a,b). The FRET area scan images of the respective microtiter well were acquired by using a multimode microtiter plate reader (BioTek synergy 2, Finland) equipped with Gene 5 software depicting the concentration dependent FRET intensity (Figure 4b). The

dx.doi.org/10.1021/ac501388a | Anal. Chem. 2014, 86, 7200–7204

FRET phenomenon between apta-immuno complex was further confirmed by performing acceptor photobleaching measurements using a 561 nm laser (100% power) for ∼80 s in a Nikon AI-R laser scanning confocal microscope. Figure 4c (i−vi) shows the concomitant increase in fluorescence intensity of the donor (FITC) with increasing concentrations of TNT in the selected ROI. The similar observations were also recorded in confocal micrographs after photobleaching experiments as shown in the insets of Figure 4c. The FRET efficiency calculated from photobleaching experiments was found to be ∼82% as calculated by the equation (FRET efficiency, $E = 1 - F_D/F_D'$),[23] where F_D and F_D' are the donor intensities before and after photobleaching the acceptor, respectively. The newly developed sensing platform using the FITC-labeled aptamer as a binder molecule while anti-TNT antibody labeled with RITC as recognition element showed excellent sensitivity ∼0.4 nM for TNT detection. The cross validation of developed apta-immuno assay with standard GC analysis (Supporting Information, Figure S8) demonstrated a high degree of correlation coefficient (∼0.993). In conclusion, we realized an apta-immunosensing FRET based platform for the detection of the explosive TNT, a security threat and environmental contaminant. A highly specific aptamer was screened using the oligonucleotide library by nanoparticles mediated modified SELEX method. The consensus moiety predicted in the selected binder sequence showed its pervasiveness in the bound state by demonstrating its stability and affinity toward the target analyte, TNT. The newly developed platform is superior in terms of its specificity and sensitivity by employing a combination of two highly selective bioreceptors tagged with FRET pair dyes in a sandwich immunoassay format. This strategy is expected to open up new opportunities for diagnosis of other smaller molecules such as pesticides, drugs of abuse, or toxins.

■ ASSOCIATED CONTENT

Ⓢ Supporting Information

Hapten design: molecular modeling, antibody generation, aptamer structure by NMR, gold nanobioprobes for partitioning of ds-DNA, control experiments. This material is available free of charge via the Internet at http://pubs.acs.org.

■ AUTHOR INFORMATION

Corresponding Author

*E-mail: raman@imtech.res.in. Fax: +91-172-2690632.

Author Contributions

[‖]P.S. and M.S. contributed equally to this work.

The manuscript was written through the contributions of all authors. All authors have given approval to the final version of the manuscript.

Notes

The authors declare no competing financial interest.

■ ACKNOWLEDGMENTS

The authors acknowledge Principal Scientific Advisor to the Government of India through DST, India for financial support and Mr. Deepak Bhatt for confocal studies.

■ REFERENCES

(1) Miura, N.; Shankaran, D. R.; Kawaguchi, T.; Matsumoto, K.; Toko, K. *Electrochemistry* **2007**, *75*, 13−22.

(2) Weiss, J. M.; McKay, A. J.; Derito, C.; Watanabe, C.; Thorn, K. A.; Madsen, E.L. *Environ. Sci. Technol.* **2004**, *38*, 2167−2174.

(3) Sulzer, P.; Petersson, F.; Agarwal, B.; Becker, K. H.; Jürschik, S.; Märk, T. D.; Perry, D.; Watts, P.; Mayhew, C. A. *Anal. Chem.* **2012**, *84*, 4161−4166. Che, Y.; Gross, D. E.; Huang, H.; Yang, D.; Yang, X.; Discekic, E.; Xue, Z.; Zhao, H.; Moore, J. S.; Zang, L. *J. Am. Chem. Soc.* **2012**, *134*, 4978−4982.

(4) Sohn, H.; Calhoun, R. M.; Sailor, M. J.; Trogler, W. C. *Angew. Chem., Int. Ed.* **2001**, *40*, 2104−2105.

(5) Dasary, S. S. R.; Singh, A. K.; Senapati, D.; Yu, H.; Ray, P. C. *J. Am. Chem. Soc.* **2009**, *131*, 13806−13812.

(6) Germain, M. E.; Knapp, M. J. *Chem. Soc. Rev.* **2009**, *38*, 2543−2555.

(7) Shangguan, D.; Meng, L.; Cao, Z. C.; Xiao, Z. *Anal. Chem.* **2008**, *80*, 721−728.

(8) Wang, Y.; La, A.; Brucknerb, C.; Lei, Y. *Chem. Commun.* **2012**, *48*, 9903−9905.

(9) Goldman, E. R.; Medintz, I. L.; Whitley, J. L.; Hayhurst, A.; Clapp, A. R.; Uyeda, H. T.; Deschamps, J. R.; Lassman, M. E.; Mattoussi, H. *J. Am. Chem. Soc.* **2005**, *127*, 6744−6751.

(10) Sapsford, K. E.; Berti, L.; Medintz, I. L. *Angew. Chem., Int. Ed.* **2006**, *45*, 4562−4589.

(11) Feng, L.; Li, H.; Qu, Y.; Lü, C. *Chem. Commun.* **2012**, *48*, 4633−4635.

(12) Lu, L. Q.; Zheng, Y.; Qu, W. G.; Xu, A.-W. *Anal. Methods* **2013**, *5*, 603−607.

(13) Sharma, P.; Bhalla, V.; Tuteja, S.; Kukkar, M.; Suri, C. R. *Analyst* **2012**, *137*, 2495−2502.

(14) Sharma, P.; Suri, C. R. *Bioresour. Technol.* **2011**, *102*, 3119−3125.

(15) Anderson, G. P.; Lamar, J. D.; Charles, P. T. *Environ. Sci. Technol.* **2007**, *41*, 2888−2893.

(16) Goldman, E. R.; Anderson, G. P.; Lebedev, N.; Lingerfelt, B. M.; Winter, P. T.; Patterson, C. H.; Mauro, J. M. *Anal. Bioanal. Chem.* **2003**, *375*, 471−475.

(17) Xiao, Y.; Lubin, A. A.; Heeger, A. J.; Plaxco, K. W. *Angew. Chem., Int. Ed.* **2005**, *117*, 5456−5459.

(18) Gandhi, S.; Caplash, N.; Sharma, P.; Suri, C. R. *Biosens. Bioelectron.* **2009**, *25*, 502−505.

(19) Priyanka; Shorie, M.; Bhalla, V.; Pathania, P.; Suri, C. R. *Chem. Commun.* **2014**, *50*, 1080−1082.

(20) Pang, S.; Labuzab, T. P.; He, L. *Analyst* **2014**, *139*, 1895−1901.

(21) Xiang, Y.; Xie, M.; Bash, R.; Chen, J. L.; Wang, J. *Angew. Chem., Int. Ed.* **2007**, *46*, 9054−9056.

(22) Korolev, N.; Lyubartsev, A. P.; Rupprecht, A.; Nordenskiold, L. *Biophys. J.* **1999**, *77*, 2736−2749.

(23) Shin, I.; Ray, J.; Gupta, V.; Ilgu, M.; Beasley, J.; Bendickson, L.; Mehanovic, S.; Kraus, G. A.; Hamilton, M. N. *Nucleic Acids Res.* **2014**, *42*, e90.